Considerations for the Thermal Modeling of Lithium-Ion Cells for Battery Analysis

Rickman, Steven L.; Christie, Robert J.; White, Ralph E.; Drolen , Bruce L.; Navarro, Moses; Coman, Paul T.

Publication date:
2016

Document version
Final published version

Document license
Unspecified

Citation for pulished version (APA):
Rickman, S. L., Christie, R. J., White, R. E., Drolen , B. L., Navarro, M., & Coman, P. T. (2016). Considerations for the Thermal Modeling of Lithium-Ion Cells for Battery Analysis. Paper presented at 46th International Conference on Environmental Systems, Vienna, Austria.

Considerations for the Thermal Modeling of Lithium-Ion Cells for Battery Analysis

Steven L. Rickman[1]
NASA Johnson Space Center, Houston, TX, 77058, USA

Robert J. Christie[2]
NASA Glenn Research Center, Cleveland, OH, 44135, USA

Ralph E. White, Ph. D.[3]
University of South Carolina, Columbia, SC, 29208, USA

Bruce L. Drolen, Ph. D.[4]
Boeing, Los Angeles, CA, 90009, USA

Moses Navarro[5]
NASA Johnson Space Center, Houston, TX, 77058, USA

Paul T. Coman[6]
Mads Clausen Institute, SDU, Sonderborg, Denmark

Recent well-publicized events involving lithium-ion batteries in laptops, electric cars, commercial aircraft and even hover boards have raised concerns regarding thermal runaway -- a phenomenon in which stored energy in a cell is rapidly released as heat along with vented effluents. If not properly managed, testing has shown that thermal runaway in a single cell can propagate to other cells in a battery and may lead to a potentially catastrophic event. Lithium-ion batteries are becoming more widely used in a number of human-rated extravehicular activity (EVA) space applications on the International Space Station. Thermal modeling in support of thermal runaway propagation mitigation in the Lithium-ion Rechargeable EVA Battery Assembly (LREBA) and the Lithium-on Pistol Grip Tool (LPGT) was pursued to inform design decisions and to understand the results of extensive development testing with the goal of enhancing safety. A correct representation of thermal runaway in battery-level thermal models requires an understanding of internal cell triggering mechanisms, heat transfer mechanisms through the cell wall, an accounting of energy transport through vented gases and effluents and proper consideration of heat transfer mechanisms within the battery. Development and refinement of internal cell multi-physics models provided heating profiles used for a simplified cell thermal network representation. A collection of simplified cells was used to formulate battery-level models of, both, the LREBA and LPGT battery configurations. Limited correlation of these models was performed using test data. An assessment of heat transport via vented gases was performed using computational fluid dynamics (CFD). Use of the models in conjunction with testing led to design enhancements for, both, the LREBA and LPGT configurations. These thermal-runaway severity-reduction measures are also being applied to other lithium-ion

[1] NASA Technical Fellow for Passive Thermal, NASA Engineering and Safety Center, 2101 NASA Parkway, Mail Stop: WE.
[2] Aerospace Engineer, Thermal Systems Branch, 21000 Brookpark Rd / MS 86-12
[3] Professor, College of Engineering and Computing, Department of Chemical Engineering, 301 Main Street, white@cec.sc.edu
[4] Senior Technical Fellow, Satellite Development Center, P.O. Box 92919, MC-W-S25-C366
[5] Mechanical Engineer, Design and Analysis Branch (EC2), 2101 NASA Parkway
[6] Ph. D. Student, Mads Clausen Institute, *Alsion 2, 6400 Sønderborg,* paulcoman@mci.sdu.dk

batteries being developed for the International Space Station, Extravehicular Mobility Unit and other programs. Modeling guidance and future efforts are discussed.

Nomenclature

A	=	Frequency factor of the reaction, in s^{-1};
fac	=	Cell heating factor;
c_p	=	Specific heat of the jelly roll, in J kg^{-1} K^{-1};
Ea	=	Activation energy of each reaction, in J;
Q_a	=	Decomposition reaction of anode, in W;
Q_c	=	Decomposition reaction of cathode, in W;
Q_s	=	Decomposition reaction of SEI, in W;
Q_{bl}	=	Heat absorbed by the electrolyte during boiling, in W;
Q_{ec}	=	Heat released due to electrochemical reactions, in W;
Q_{ej}	=	Heat carried by ejecta, in W;
Q_{cnv}	=	Heat dissipating through convection, in W;
Q_{rad}	=	Heat dissipating through radiation, in W;
T	=	Average cell temperature, in K;
V_{cel}	=	Volume of the cell, in m^3;
i	=	Index corresponding to reactions in anode, cathode and SEI;
k_b	=	Boltzmann constant, in J K^{-1};
t	=	Time, in s;
x	=	Fraction of Li intercalated in each battery component;

I. Background

Advances in battery technology have led to ever-increasing specific energy (W-hr/kg) and specific power (W/kg). Today's secondary (rechargeable) lithium-ion batteries have demonstrated specific energies in the 100-200 W-hr/kg range with demonstrated specific powers as high as 500 W/kg. Older aerospace systems used battery chemistries such as nickel-cadmium with about four times less specific power and nickel-hydrogen with about two times less specific power. These batteries also had thermal challenges when they were first introduced but the thermal challenges with lithium-ion cells are even more severe due to the higher energy density. The excellent, mass-efficient, energy storage capability of lithium-ion batteries has led to their use on many aerospace platforms and on countless diverse commercial products including laptops, electric cars and more recently hover boards. Many recent events have been reported where lithium-ion cells rapidly released their stored energy leading to fires. This phenomenon is referred to as thermal runaway (TR). While TR of a single cell in a system's battery pack remains a significant event that needs to be accounted for in the system design, such an event can be more readily contained without significant ramifications. However, when TR of a single cell triggers the subsequent TR of an adjacent cell or cells this leads to a propagating event that has even more serious system impacts. The focus of this paper is on development of analysis and design capabilities to drive toward lithium-ion batteries that preclude thermal runaway propagation of a cell failure within a battery pack.

By way of example, consider a typical commercially available lithium-ion 18650 cell (cylindrically-shaped with an 18 mm diameter and 65 mm long) slightly longer and fatter than a conventional AA battery. The specification sheet for such a cell might list its nominal capacity as 2.6 Amp-hours with a average voltage of 3.7 V. A typical mass for such a cell would be just under 50 grams. The electrical energy stored in the cell at the nominal voltage is then 2.6 × 3.7 = 9.62 W-hrs = 34,632 J. The cell's thermal mass can be estimated by the product of its mass and the effective specific heat of the constituent materials which is often reported to be close to 0.9 J/g-ºC, slightly lower than that of one of the major constituents, aluminum, which has a specific heat of 0.95 J/g-ºC. The typical thermal mass for such an 18650 rechargeable lithium-ion cell is then 45 J/ºC. Assuming that during a cell TR event, all of the stored electrical energy converts to heat and it all works to warm the mass of the cell, the temperature rise of the cell during such an event can be estimated by dividing the total stored electrical energy by the thermal mass. The estimated temperature rise for the typical 18650 lithium-ion cell described above would be (34,632 J)/(45 J/ºC) = 770ºC. Assuming an initial temperature of, say 30ºC, leads to a predicted maximum cell temperature in such an event of about 800ºC.

In a real system/battery there are heat loss paths from the cell including heat conduction to adjacent cells and structure, convection to the air in the battery, if present, and radiation to the cell's surroundings. Designing a system to remove the heat from a cell going through thermal runaway quickly enough to avoid this temperature rise is in most

cases prohibitive. Often the majority of the energy release during a cell TR occurs in as little as 10-20 s. To address such a rapid heat loss would require a cooling system capable of removing roughly 3000 W from any one cell in the battery at a heat flux of more than 500,000 W/m^2. This heat load is three or more orders of magnitude higher than the typical heat dissipation of any one cell during normal operation of the system and the heat flux far exceeds the capacity of most available means of cooling. Incorporation of such cooling systems would lead to huge cooling mass penalties that would far offset the gains made by use of such mass efficient batteries. A more practical path is to design batteries that can experience the TR of a given cell in the pack without deleterious system effects and without propagation of the event to other cells in the battery. Given that 800ºC is a high enough temperature to melt the aluminum (about 660ºC) and leads to many other chemical reactions within the cell, accurate prediction of the actual peak temperature of the cell and the effect of this hot cell on its neighboring cells is much more complicated than the simple estimates made here and is the subject of much of what follows. Suffice it to say that addressing the possibility of a cell in a battery pack reaching such high temperatures must be the focus of significant design, analysis and test before the fielding of safe lithium-ion batteries.

The basic scenario for a propagating event is that the TR of a given cell in a battery pack leads to extremely fast warming of its internal cell windings followed closely by the cell's case. This then warms the case of a neighboring cell which in turn warms its winding. When the neighbor's winding warms up sufficiently, the plastic separator material that separates the anode and cathode layers in the cell will melt allowing the anode and cathode to come into contact leading to a short within this adjacent cell and, in turn, lead to the TR of the neighboring cell. When a cell experiences TR the sources of energy include not only the stored electrical energy but also the exothermic energy released in the various chemical reactions triggered by the high temperatures including combustion within the cell fed by oxygen released form the cathode materials. As the cell temperature increases the vapor pressure of the electrolyte within the cell also increases. When the internal pressure exceeds the maximum pressure of the vent port of the TR cell, its vent opens and vented gas carries significant energy away from this cell which can impinge upon neighboring cells. Additionally, the TR cell presents an external short to any parallel cells, whose warming increases their propensity to TR propagation. All of these effects, and more, must be considered to simulate accurately the effects of a thermal runaway and the likelihood of propagation of such an event to an adjacent cell.

Thermal modeling in support of thermal runaway propagation mitigation in the Lithium-ion Rechargeable EVA Battery Assembly (LREBA) and the Lithium-ion Pistol Grip Tool (LPGT) was pursued to inform design decisions and to understand the results of extensive development testing with the goal of enhancing safety. While batteries used for International Space Station (ISS) applications are considered safe due to extensive cell screening, low use profiles, and fault-tolerant hazard mitigations, efforts are under way to further improve the safety as the program pursues additional, affordable risk reductions and by addressing the consequence should a very unlikely failure occur. Analysis of battery configurations considered for risk reduction activities are discussed in this paper.

II. Introduction

Development and maturation of the Lithium-ion Rechargeable Battery (LREBA) and the Lithium-ion Pistol Grip Tool (LPGT) battery designs relied not only on testing but, also, thermal and fluids analysis. The overall flow is presented in Figure 1.

A representation of a single cell internal model was formulated using the COMSOL Multiphysics®[7] software and used to estimate heat generation due to thermal runaway. Confirmation of the cell energy content was pursued using Accelerating Rate Calorimetry (ARC). Internal heating rate estimates resulting from thermal runaway were used to formulate a detailed single cell thermal model which was subsequently used as an element of higher-level battery thermal radiation and network models of, both, the LREBA and LPGT battery configurations. Computational Fluid Dynamics (CFD) analysis of the LPGT configuration was also performed to assess the heat transport via vented gases within the battery enclosure.

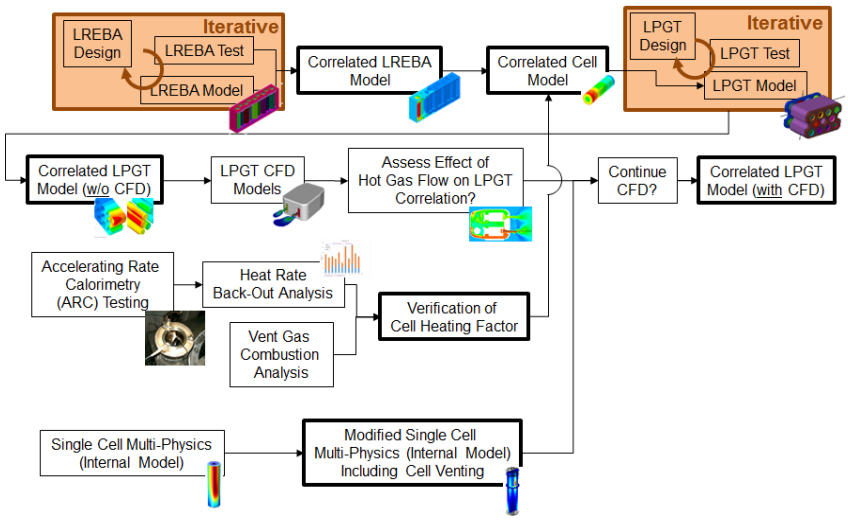

Figure 1. A summary of cell and battery analyses.

III. Mathematical Modeling

Although numerical modeling of the propagation of thermal runaway from one cell to another is very important, a key to this modeling is accurately tallying the total energy that is released during thermal runaway in a single cell, as well as the energy that is leaving due to venting of ejecta. Moreover, the importance of including venting during modeling of thermal runaway is investigated. Having such a model will provide a better evaluation of the energy balance and the state functions needed for a CFD model. The model, described in detail by Coman et al. in Ref. 1, consists of different ordinary differential equations (ODEs) representing the reaction rates and the isentropic flow equations during the venting event. The reactions rates are given in Arrhenius form, as follows:

$$\frac{dx_i}{dt} = -A_i x_i \exp\left(\frac{-\mathrm{Ea}_i}{k_b T}\right) \tag{1}$$

where x is the fraction of Li intercalated in each battery component, represented by the index (i), which corresponds to the reactions occurring in the anode, cathode and solid-electrolyte interphase (SEI) layer. The terms t, A, Ea, k_b and T represent the time, frequency factor, the activation energy, the Boltzmann constant and the temperature of the battery, respectively. Detailed descriptions of the different decomposition reactions in the anode, cathode and the SEI are described by Dahn et al.[2]. The boiling of the electrolyte and the energy released due to electrochemical reactions (given by the State of Charge) are also included in the modeling and they are described with the same Arrhenius form with extra terms, as described in Ref. 1. The activation energies and the frequency factors were fitted to data in order to account for some of the other reactions (known and unknown) that are not included in the model.

For the venting event, the flow equations for the ejecta venting (parts of the jelly roll and the electrolyte) are formulated considering an isentropic flow regime. The equations used for such a regime are summarized in Ref. 3, while the theory can be found in Ref. 4. By modeling the flow during thermal runaway, the pressure, the temperature and the velocity of the effluent will be evaluated. For the state functions and the velocity, an initiation condition is considered as the point where the pressure equates to the pressure limit of the venting disc.

The total heat source consists therefore of the different processes and it is used in the energy balance for evaluating the temperature of the battery, as follows:

[7] COMSOL Multiphysics® is a registered trademark of COMSOL, Inc.

$$V_{cel}\rho(y)c_{p,jr}\frac{dT}{dt}=\sum_i Q_i \tag{2}$$

where

$$\sum_i Q_i = Q_a + Q_c + Q_s + Q_{cnv} + Q_{rad} + Q_{ec} - Q_{ej} - Q_{bl} \tag{3}$$

The terms from Eq. (2) represent the volume of the cell (V_{cel}), the density of the jelly roll (ρ), which is a function of the mass fraction that leaves the cell with the ejecta (y) and the specific heat of the jelly roll ($c_{p,jr}$). The terms in Eq. (3) represent the heat contribution due to the exothermic decomposition of the anode, cathode and SEI layers (Q_a, Q_c and Q_s), the heat contribution due to convection and radiation (Q_{cnv} and Q_{rad}), the exothermic electrochemical reactions (Q_{ec}) and the endothermic effects of boiling (Q_{bl}). The energy leaving the system is carried by the ejecta and is also included in the heat balance (Q_{ej}).

With a comprehensive tally of the system energies, it is possible to use the model to predict the temperature inside the battery. Moreover analyzing the fractions of Li in the different components gives a better understanding of the processes that occur inside. The model was validated against the experiments performed in Ref. 5, where the authors heated the battery in an oven with a temperature slope of 2ºC/min. The comparison can be seen in Figure 2 for two different cases – with venting and without venting. Considering that the model is lumped, the temperature reported is the average temperature over the entire jelly roll, while the experimental temperature is read by a thermocouple affixed to the cell can.

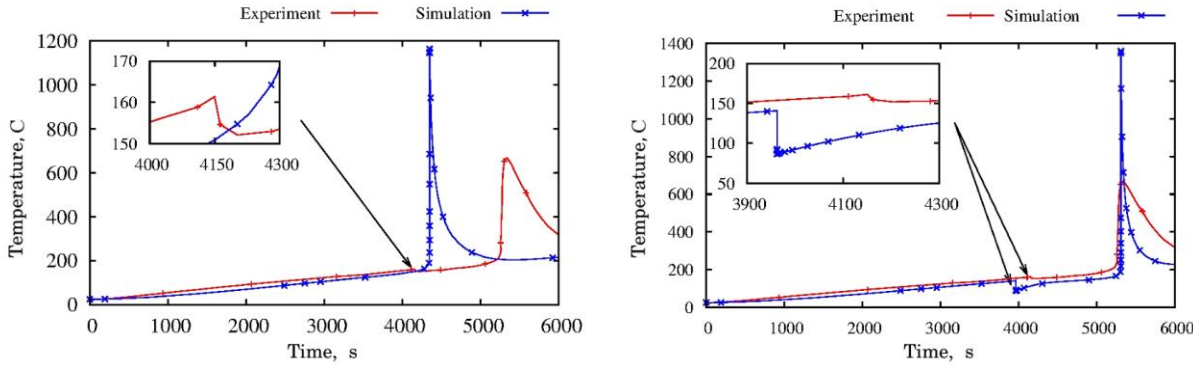

a) b)

Figure 2. A comparison of model predicted temperatures to experimental measurements from Ref. 5 during oven heating with a temperature slope of 2ºC/min a) without venting and b) with venting.

From Figure 2 a) one can see that if the system is modeled without using the flow equations (no venting), the thermal runaway evaluated experimentally is initiated around the point where venting occurs. This means that at that point, the pressure reached the safety disc burst pressure, leading to venting of ejecta. If the pressure and, implicitly, a venting condition are not considered, the model fails to evaluate the right dynamics. However, when venting is included in the model, the model predicts the correct behavior. From Figure 2 b), one can see that the temperature drops around the point where the experiments read the temperature drop. This drop is caused by the venting of some gas. After this point, the temperature recovers due to the continuous exposure to the oven temperature and continues to heat until the onset temperature of the thermal runaway is reached, leading the system to thermal runaway. After this point, there are some slight differences in the cooling slope caused by the difference in the peak temperatures as well as by the numerical resolution and perhaps other assumptions such as the assumed thermal resistance between the winding and the steel case of the cell.

By comparing Figure 2 a) with Figure 2 b), one can observe the importance of having the flow equations included in the model. Moreover, if no pressure condition is applied, the model fails to tally the amount of heat leaving the cell, which can cause significant errors when evaluating the cell temperature.

IV. Simplified and Detailed Cell Thermal Models

Initial analysis efforts focused on modeling single cell thermal response observed during testing of the 18650 cell configuration. In the simplest configuration, the 18650 cell was represented as a homogeneous thermal mass with representative density, specific heat and thermal conductivity. A heating profile from an early detailed internal cell multi-physics analysis was added to the cell model and included the heat generation due to ohmic heating as well as chemical reactions within the cell. Logic within the model was used to trigger the thermal runaway simulation when any cell node reached a specified trigger temperature. While this approach was successful in modeling some gross characteristics of the cell thermal response, the homogeneous nature of the simplified cell representation precluded modeling the effect of heat soak and the associated time delay into the jelly roll region. Use of the model in this form would have complicated the modeling of cell pre-heating which was used to trigger thermal runaway during testing. Additionally, the thermal runaway trigger could only be specified based on an external surface temperature criterion.

By enhancing the cell thermal model as shown in Figure 3, it became possible to correlate cell exterior can temperatures with test data, investigate the interface conductance between the cell can and the jelly roll and model the jelly roll heat generation. Direct measurement of jelly roll temperatures leading up to and during thermal runaway was not possible as no internal temperature measurements were available. Therefore, a determination of whether the cell thermal model was reasonable could only be made based on externally observable events and/or post-test evidence and included matching the cell pre-heating rate and time to trigger thermal runaway observed during testing, measurement of the cell can peak temperature during the thermal runaway and post-test inspection of the cell carcass to determine whether the melting temperatures of aluminum or copper were reached. Post-test investigation of the cell carcass indicated that the jelly roll had achieved temperatures in excess of the aluminum melt temperature (660ºC) but less than that required to melt copper (1,085ºC).

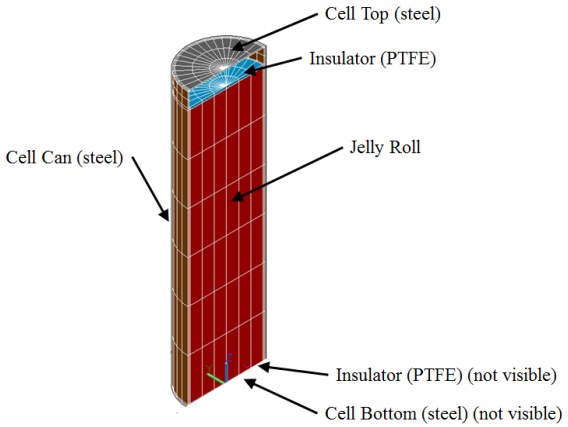

Figure 3. A detailed 18650 cell thermal model (cut-away view).

Internal cell heat generation during thermal runaway is a combination of ohmic heating and heating resulting from chemical reactions within the cell. During thermal runaway, the majority of heat generation occurs over a very short time period, on the order of 20 s. The area under the heating rate versus time curve is the total heat energy liberated during the thermal runaway event. A proper accounting of energy liberation is key to establishing a suitable thermal model.

The detailed cell model included separate representations of the cell can, top, bottom, jelly roll, internal insulators, and representations of the conduction paths from the jelly roll to the cell top and bottom terminals. The interface conductance between the cell can and the jelly roll was estimated through correlation of, both, the cell preheat time involving the heat transfer path from the cell can surface *into* the jelly roll and the observed time of peak cell can temperature as heating generated within the jelly roll conducted *out of* the cell.

It is important to note that a number of simplifying assumptions were required when formulating the cell model to render the analysis tractable. Aside from mass loss due to venting, the cell was assumed to stay intact throughout the analysis – that is, the cell geometry and heat transfer paths remained intact even though thermal runaway had taken place. Examination of cell carcasses post-test indicates that this is not a good assumption as the cell geometry changes including expulsion of cell effluents and even the jelly roll in some instances. Additionally, melt products may alter heat transfer paths. These shortcomings may inhibit model correlation in some cases.

V. Battery Level Thermal Models

Battery level thermal models were developed for, both, the LREBA and LPGT configurations that utilized multiple instances of the detailed cell thermal model originally developed for the LREBA analysis. The Thermal

Desktop®[8] suite of analysis tools was used to formulate a Systems Improved Numerical Differencing Analyzer/Fluid Integrator (SINDA/FLUINT) thermal network model from which temperatures were calculated. The models were subsequently correlated to thermal test data and are described in the following sections.

A. Lithium-Ion Reusable Battery (LREBA) Thermal Model

As the LREBA design evolved, numerous thermal models were developed to better understand the contribution of heat transfer mechanisms within the battery enclosure.

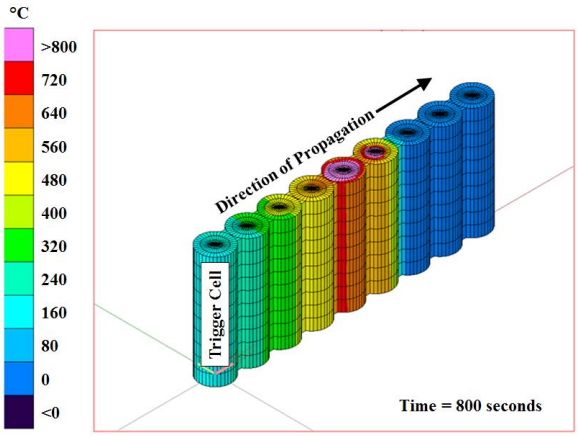

Figure 4. 18650 cells in the 9P "picket fence" configuration.

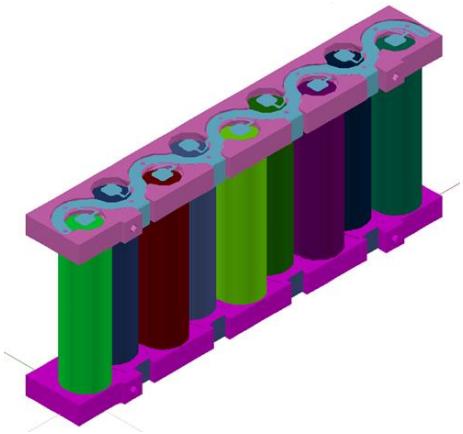

Figure 5. The modified 9P configuration showing the separated, staggered cell arrangement.

Initial analyses focused on thermal runaway propagation as observed for the 9P "picket fence" configuration testing depicted in Figure 4. The initial cell modelling effort assumed no venting and resulted in all heat generated within the jelly roll conducting to the cell can side, top and bottom. For the array of cells depicted, the analysis assumed intact cells with heat transfer to adjacent cells via conduction and radiation. However, testing showed clear evidence of venting and effluents and the combustion of vent products with atmospheric air. The model consisted of nine single cell models with an epoxy fillet between each pair of cells creating a conduction path. Thermal radiation and natural convection from all free surfaces was modeled. For a single cell trigger, the analysis predicted propagation of thermal runaway to all cells in the 9P. Burning vent products provided additional heating which was not modeled and it was assumed that all mass was retained and that all energy left the cell through the cell can structure via conduction, convection and radiation. Subsequent analysis and test correlation to battery-level testing confirmed that too much energy was assumed to be retained in the cell and the need for scaling the amount of heating permeating the cell can wall was realized.

The direct contact between cells in the 9P configuration was deemed unacceptable and subsequent designs featured cell to cell separation facilitated by adding a stand-off distance and a staggered cell configuration, a non-metallic capture plate and bus plates with reduced cell-to-cell thermal conduction capability. This configuration is depicted in Figure 5.

As evidenced by the single cell, 9P and LREBA-level testing, the vented effluents and their propensity to combust was an important factor in whether or not thermal runaway propagated. Alternate LREBA configurations were devised and tested. Configurations in which the effluents were vented out of the LREBA enclosure resulted in tests with no propagation. To represent this facet of the design in the LREBA analysis, a cell heating factor ($0 \leq fac \leq 1$) was devised and represented the fraction of the energy that remained within the cell can. Conversely, the fraction of the total cell energy vented from the enclosure is given by:

$$fraction\ of\ energy\ vented = (1 - fac) \tag{4}$$

It is emphasized that implementation of the cell heating factor is an oversimplification of possible outcomes of a thermal runaway event.

[8] Thermal Desktop® is a registered trademark of Cullimore and Ring Technologies, Inc.

When the LREBA chassis design was modified to include direct venting of effluents outside of the battery enclosure, thermal analysis of the configuration was greatly simplified and could be reasonably expressed using only conduction through LREBA components, air conduction and radiation.

For the LREBA thermal analysis, a representative segment of the dog-leg section was modeled and is depicted in Figure 6.

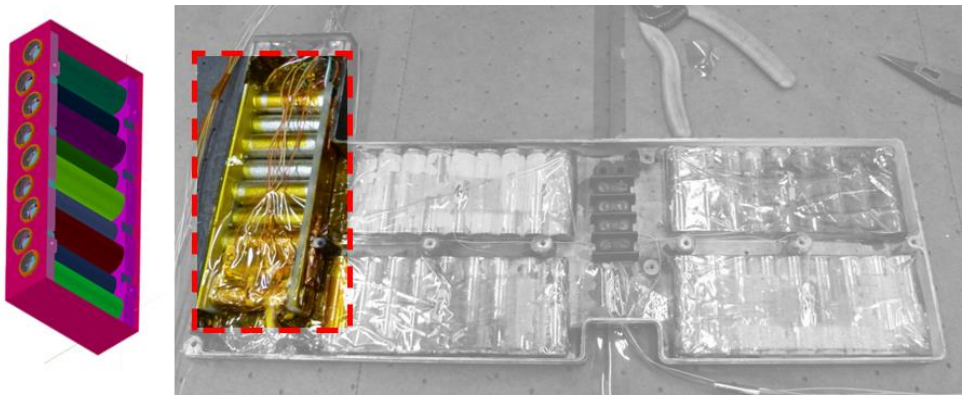

Figure 6. Representative 9P segment thermal model in relation to the full LREBA configuration (lid removed in, both, the thermal model and the test unit for clarity).

An external convective heat transfer coefficient of 7 W/m^2-ºC was assumed for all surfaces and falls within the range of natural convection. The ambient air temperature was used for, both, the convective and radiative boundary condition. Thermal radiation to the ambient environment was modeled for the enclosure surface nodes except for those on the side resting on a tile surface during testing. In this case, the model included radiation to the tile temperature, assumed to be 29.5ºC, a value representative of the ambient environment.

The detailed single cell model was utilized and CAD geometries were meshed into a finite element model (FEM) representation of the analysis geometry using Thermal Desktop's® TD mesher function. The heating rate versus time profile used to simulate thermal runaway was taken from an early COMSOL Multi-physics® simulation and included the effects of, both, ohmic heating and chemical reactions within the cell.

Model correlation first assumed a high heat exchange with the air within the enclosure but this was not physically valid as it would require unrealistic convective heat transfer coefficients. Given that considerable mass was ejected during a thermal runaway event, it was reasonable to assume adjustment of the cell heating factor to allow correlation of temperatures observed on the trigger cell. Ultimately, the best correlation for trigger cell temperatures suggested that less than 50% of cell energy emerged through the cell can wall. While this produced good correlation in the vicinity of the trigger cell, temperatures at the far end of the dog leg did not correlate well to test data. Subsequent refinement of the model included a detailed representation of the air volume to permit heat transfer via air conduction and this increase in model fidelity dramatically improved correlation to test data at the far end of the dog leg enclosure. The small spacing within the battery enclosure supports simulating heat transfer via the air paths as conductive rather than via natural convection.

After initial checkout runs, the LREBA thermal model was correlated to test data on a configuration that was representative of many of the features of the final design.

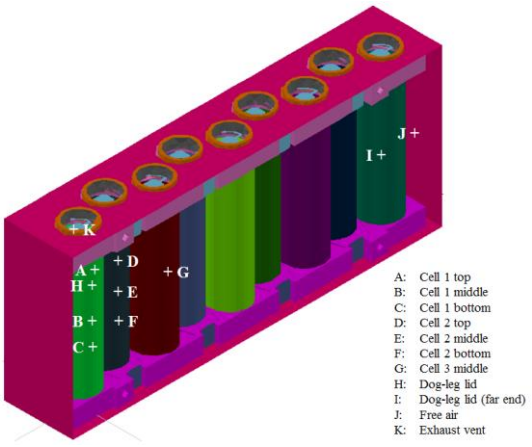

Figure 7. Locations used for model correlation with lid removed for clarity.

The test configuration is depicted in Figure 7 and annotated with locations corresponding to approximate thermocouple locations depicted.

A comparison of test data and the correlated thermal model is presented in Figures 8 - 15. The correlation plots are divided into two groups: the first group, consisting of eight measurements, depicts results where model correlation was considered good to excellent, the second, consisting of only three measurements, did not show good correlation.

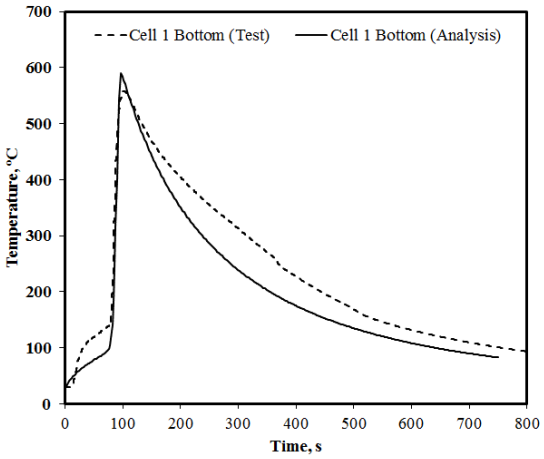

Figure 8. Cell 1 (trigger cell) bottom.

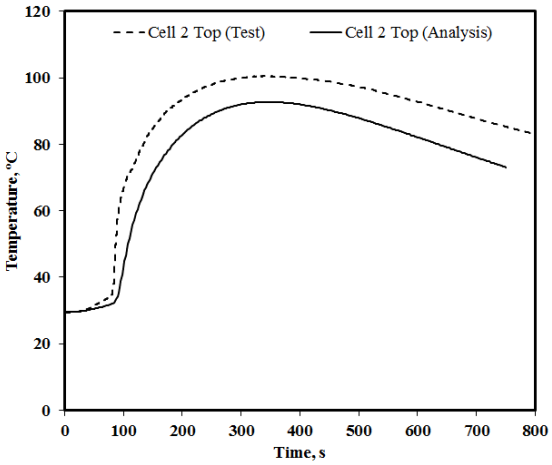

Figure 9. Cell 2 top.

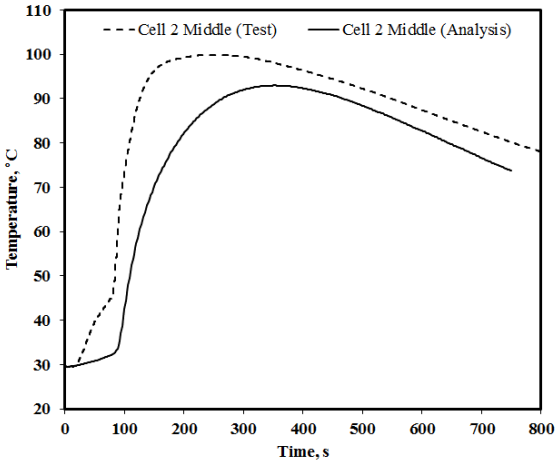

Figure 10. Cell 2 middle.

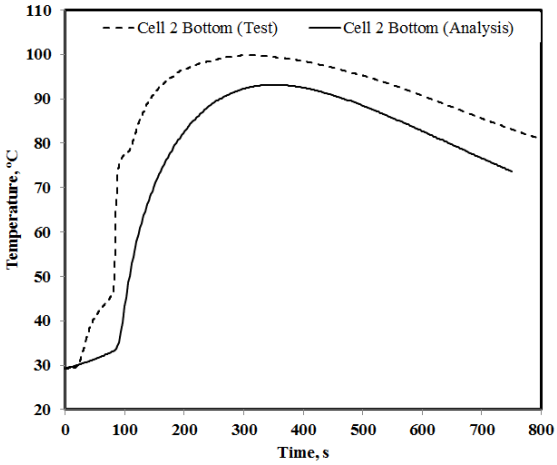

Figure 11. Cell 2 bottom.

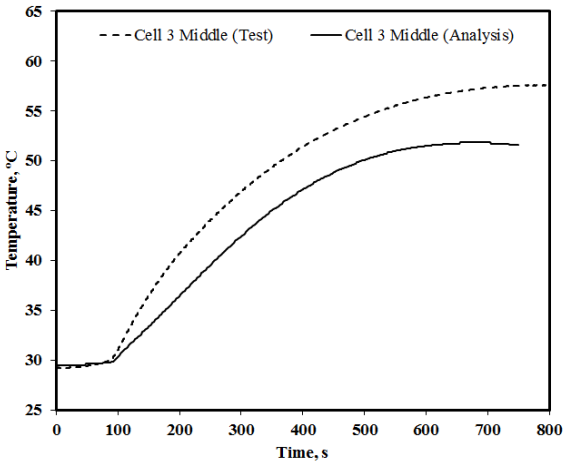

Figure 12. Cell 3 middle.

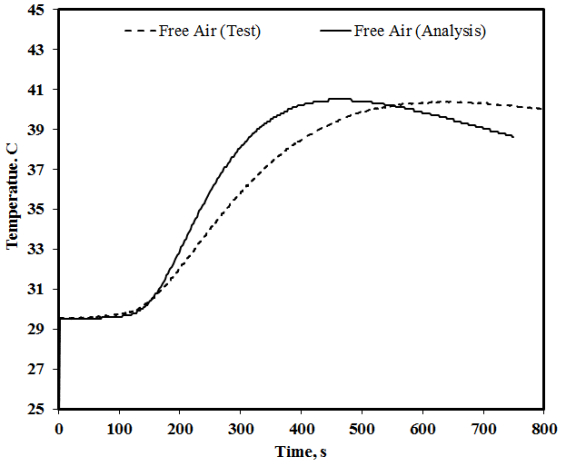

Figure 13. Free air inside dog-leg.

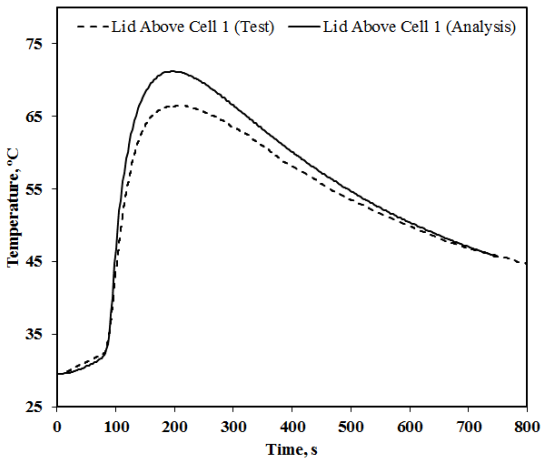

Figure 14. Dog-leg lid (above trigger cell).

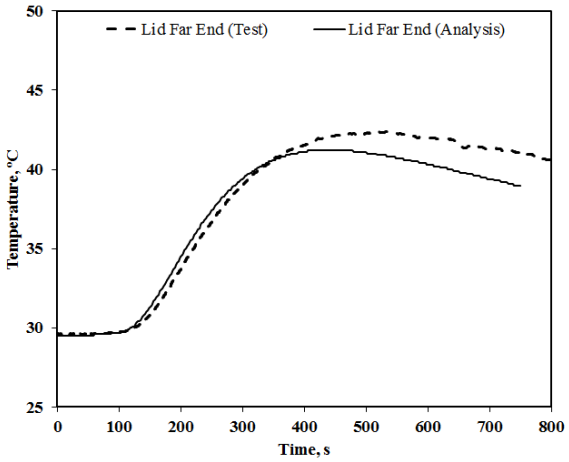

Figure 15. Dog-leg lid (far end).

Correlation for the Cell 1 (i.e., the trigger cell) middle (Figure 16) and top (Figure 17) was considered poor and may be attributable to thermocouple bonding and/or the assumed interface conductance between the cell top and the capture plate. It should be noted that correlation of the Macor®[9] exhaust vent pipe, not shown, was complicated by the unknown state of the measurement as the rapid response suggested that the thermocouple had become disbonded from the vent pipe and, therefore, was more a measure of vent gas temperature. Nonetheless, the correlation produced good results for heating to adjacent cells which is key to understanding the propensity of a thermal runaway to propagate to other cells in proximity to the trigger cell.

[9] Macor® is a registered trademark of Corning, Inc.

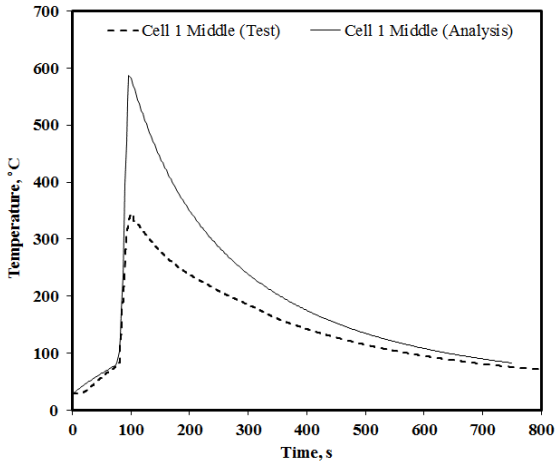

Figure 16. Cell 1 middle (trigger cell).

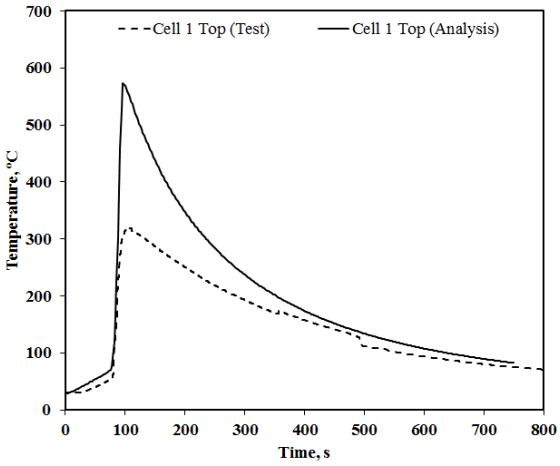

Figure 17. Cell 1 top (trigger cell).

With successful model correlation, the detailed cell model used within the LREBA model for heat spreader analysis as well as the LPGT model is described in the following sections.

B. LREBA Model with Heat Spreader

To direct the heat from a trigger cell to the enclosure and away from an adjacent cell, a heat spreader was incorporated. The heat spreader, as shown in Figure 18, is made of aluminum and has thermally conductive Gap Pad®[10] to improve thermal conductance at the interfaces between the cells and the spreader and between the spreader and the enclosure. Both the upper and lower spreaders are only in contact with every other cell; thus there is more thermal resistance between cells than there is between the cells and the enclosure. Mica sleeves were also wrapped around the cells. These were originally intended to provide electrical insulation, i.e. to prevent ejecta from causing electrical shorting between the cells. It was later found that the mica sleeves helped to confine heat to the trigger cell and thus helped to impede thermal runaway of adjacent cells. Thermal sub-models of the upper and lower spreaders were incorporated into the LREBA thermal model. Interstitial air conduction was previously found to be an important factor during model correlation, so a model of the interstitial air was also added. Initial analysis showed that the spreader was absorbing significant heat from the pre-heater which was used during testing to initiate thermal runaway; therefore, guidance was provided to the test team to guide the wattage needed for a successful test.

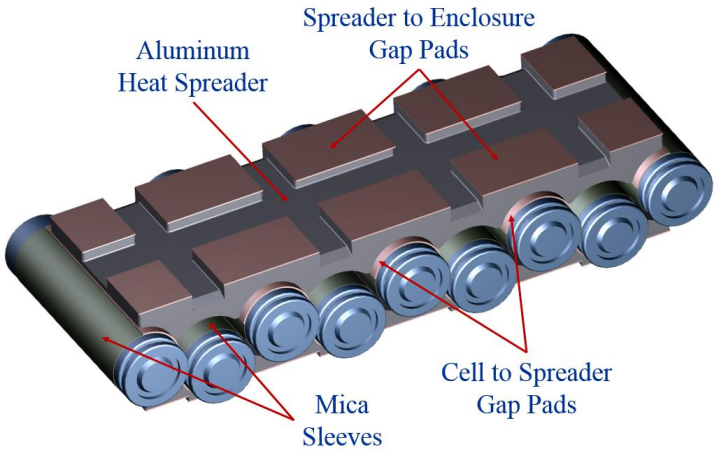

Figure 18. LREBA battery pack with heat spreader added.

Figure 19 shows a typical cell temperature plot of the LREBA battery pack during a thermal runaway. The temperature scale on the left is for Cell 1 (the trigger cell) and the scale on the right is for the adjacent cell, Cell 2 and the subsequent cell, Cell 3. Although program schedule did not allow for a formal correlation with test data, the results are consistent with those observed during testing. The double-headed arrow shows the time lag between hottest temperature for Cell 2 and the thermocouple location for that cell. The difference between the two highlights that the test thermocouple is located at a relatively cool location on the cell. The hottest jelly roll temperature for Cell 2 is

[10] Gap Pad® is a registered trademark of The Bergquist Company

also shown. The jelly roll temperature is the one that determines if thermal runaway propagation will occur. Note that it is nearly 30ºC warmer than the test thermocouple temperature which is located on the 'can wall bottom'.

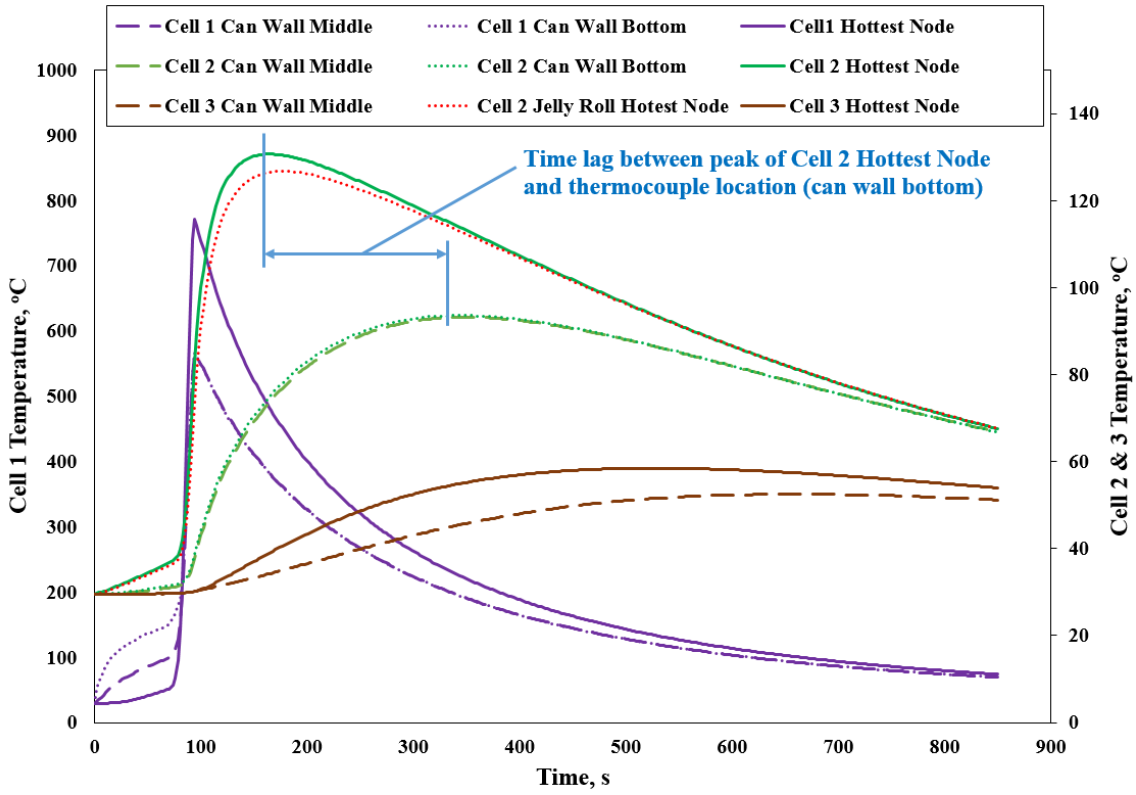

Figure 19. LREBA battery pack temperatures during thermal runaway.

Analyses were also performed to evaluate the overall benefit of adding the spreader. The cell heating factor (*fac*) determines how much heat energy remains in the cell versus being ejected. To determine the benefit of the spreader, the *fac* was increased until thermal runaway propagation occurred with and without the spreader. Starting with a *fac* of 0.37 (a number derived from LREBA testing) it was increased in increments until thermal runaway propagated from the trigger cell to the adjacent cell. Without the spreader, propagation occurred at a *fac* of 0.90 and with the spreader it occurred at 0.95. This indicated that the design without the spreader was already rather robust and including the spreader only added a small margin. The spreader likely serves better at providing physical protection from hot ejecta rather than thermal conduction protection.

C. Lithium-Ion Pistol Grip Tool (LPGT)

Thermal analysis was also performed on the battery-pack of the Li-Ion Pistol Grip Tool (LPGT). The battery pack consists of ten 18650 lithium-ion battery cells which are held together by two capture-plates, as shown in Figure 20. The thermal model simulated the LPGT Battery Pack and was developed using Thermal Desktop®. The thermal models of the cells were simply taken from the LREBA model described in the previous section. The model is mainly a heat conduction model but does include cell-wall radiation-exchange. A computational fluid dynamics (CFD) model was also created which was used to generate heat flux loads transported by vented gases for application to the exposed surfaces of the battery pack. The CFD analysis is described in the following sections.

A comparison with test data was performed which found that the analytical results for the trigger cell tracked the test data rather well: both peaked at about 570ºC and during cool down both passed through 300ºC at about 400 s. On the other hand, the analytical results for the adjacent cell temperatures were quite low. Shortly after thermal runaway the warmest cell reached only 40ºC whereas the test data peaked at 70ºC. Furthermore, after a long period the adjacent cell temperature remained low. This is an indication that the applied heat flux was too low. After several iterations it was found that a much better correlation can be obtained if the heat flux transported via vented gas is increased by a factor of 3 or 4, depending on the duration of the applied load.

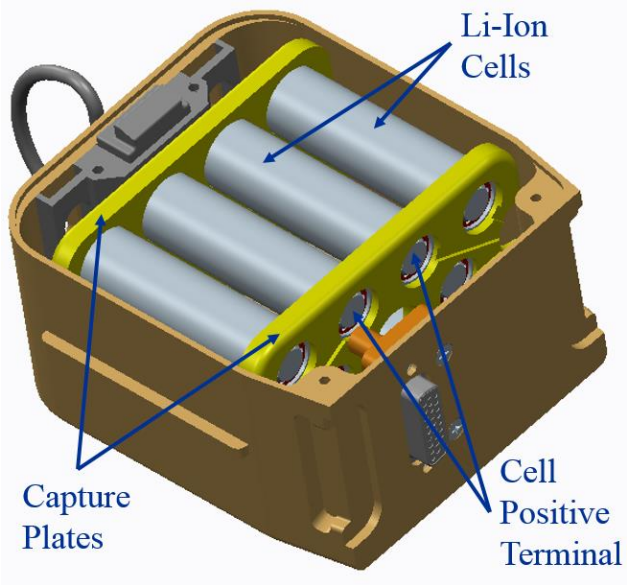

Figure 20. LPGT battery pack.

The cell numbering for the battery pack is shown in Figure 21. The trigger cell is Cell 10. A close-up of the adjacent cell temperature response after thermal runaway of the trigger cell is shown for the test and the model in Figure 22. It was found by trial and error that if the CFD-generated heat flux was multiplied by 4 the temperature of the peak would better match the test results. Although the initial peaks matched, the width of the time response was very different: The analytical model response was much narrower. It was suspected that the CFD load was not being applied for a long enough period. Test data showed that the pressure in the housing rose and fell within 4 s, therefore in the initial analysis the CFD load was only applied for that amount of time. But, there was also a thermocouple in the free air volume of the housing. When the cells vent they do so directly into this volume, thus this is a good location to monitor vent activity. The test data showed that it took about 7 s for the sensor to reach peak temperature. After that, the venting likely tapered off gradually. Therefore, instead of having just a 4 s heat load pulse, an additional 6 s taper-off period was added, and since the load period was extended, the multiplication factor on the heat flux was reduced from 4 to 3. It is hypothesized that the adjustment of CFD-generated heat fluxes is required because, while the CFD tallies the convective transfer from the vent gases, it does not account for the heat transfer caused by hot particulates, condensing vapors and liquids, flames, sparks, etc. that are also present in a thermal runaway event. Improvement is

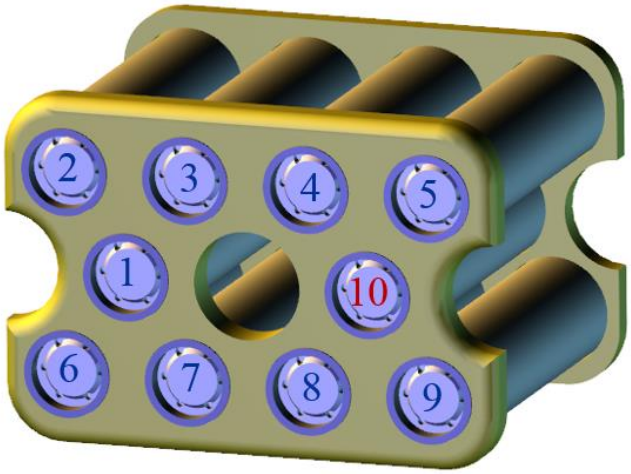

Figure 21. LPGT cell numbering.

expected once particulates are included and other model enhancements are added such as improved knowledge of the cell canister to jelly roll interface conductance.

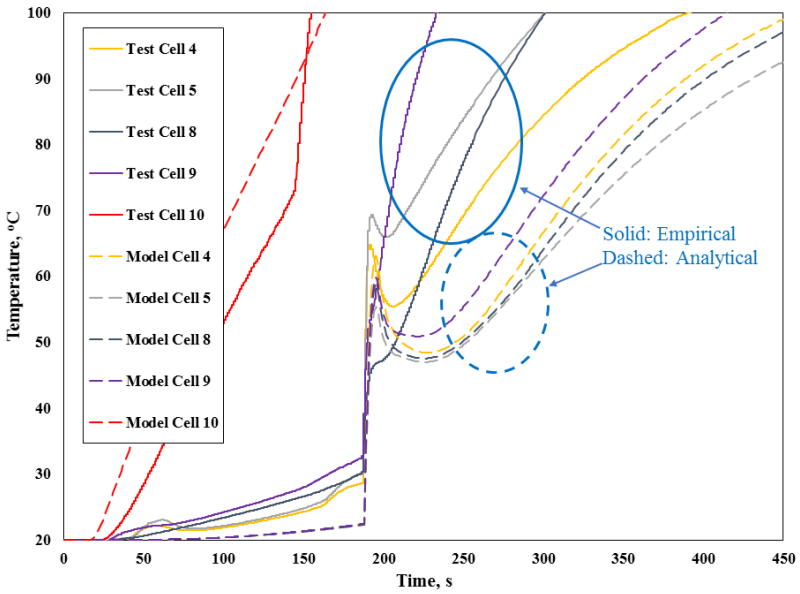

Figure 22. Adjacent cell temperature responses.

Even after modifying the CFD-generated heat flux load, the adjacent cells reached peak temperature approximately 250 s after thermal runaway occurred whereas the model predicted 400 s. So, either the rate of heat transfer is too low or the thermal capacity is too high or both. Recent measurement of the cell wall thickness found that the cells have a wall thickness of 160 μm whereas the model was using 300 μm. Model response improved after the thickness correction but there was still a significant difference in response time. The cell to air contact conductance was also increased to 1000 W/m^2-°C, which is consistent with what was used in the LREBA model. Figure 22 shows the test data superimposed on the model result, after all of these changes were made. These show that after thermal runaway the test data for the adjacent cell temperatures still rise much more rapidly between 200-300 s. It is not obvious how this additional heat is getting to the cell wall during the test. Some possibilities include:

- The enclosure was not included in the thermal model. As modeled, the battery pack is surrounded by an adiabatic environment. If the enclosure had been included, radiation would have been reemitted from the enclosure walls thus producing more paths for heat transfer back to the cells.
- The cell can wall to jelly roll contact conductance might be too high, thus allowing heat to be absorbed into the jelly roll too soon.
- The thermal capacitance of the jelly roll may be too high.
- Natural convection may need to be added.
- The mica overwrap and its effects may not be properly accounted for.
- Even though the final temperatures are similar, the test article may have more energy than what the model accounts for. The additional energy heats up the cell quickly but dissipates to and through the enclosure later on. This would explain why temperatures are higher between 200 – 300 s but not later.
- The thermocouple wires were not thermally insulated. The heat flux load would have warmed the leads significantly and that heat could cause a local hot spot.

It is suspected that cell can wall to jelly roll contact conductance is too high and cell-focused tests are needed to refine this value.

D. LPGT CFD Models

A CFD model was created for the LPGT battery from the CAD model shown in Figure 23. During a thermal runaway event for this design, gas is vented from a given cell(s) and is then routed through passages. The gas mixture is eventually vented through the four enclosure vents, also shown in Figure 23. Pre-processing of the geometry was performed with ANSYS® DesignModeler™ [11] and meshing was performed with ANSYS® Meshing™ [12]. The screens at the enclosure exit vents were modeled as a porous media. The screen domains were assumed to be 1/16 inch thick and were assumed to have an isotropic permeability value of 7.05×10^{-12} m^2. Numerical simulations were performed with ANSYS® Fluent®[13]. The steady-state solver was used for the simulation, which was chosen due to the large clock-time associated with running a transient solution. The gas mixture venting from the battery was assumed to be composed of the species and their respective concentrations listed in Table 1 (Ref. 6). For the viscous model the analysis assumed the k-epsilon (k-ε) standard scalable wall function (WF) model. A mass inflow boundary condition was prescribed at the vent surfaces for the trigger cell (Cell 10), which was the battery cell assumed to be in thermal runaway. The simulation assumed the trigger cell was venting gas at a rate of 0.001525 kg/s and at a temperature of 1419 K (1146 ºC). The wall surfaces within the battery enclosure (housing, battery cells, etc.) were assigned a constant temperature boundary condition of 300 K (27 ºC). This temperature wall boundary condition is representative of the hardware initial temperature prior to thermal runaway. In reality the wall surfaces have a finite amount of thermal mass and will therefore not stay at a constant temperature. Therefore, the simulation results are representative of some finite amount of time; a time large enough for the flow to become quasi-steady, but short enough that wall surfaces have not increased in temperature by large amounts.

Table 1. Assumed Vent Gas Composition

Species:	H2	CO2	CO	C2H4	CH4	C2H6
Gamma	1.41	1.28	1.4	1.24	1.32	1.1939
Molar Mass	2.016	44.01	28.011	28.054	16.044	30.069
Volume Fractions (%)	30	24.9	27.6	7.7	8.6	1.2

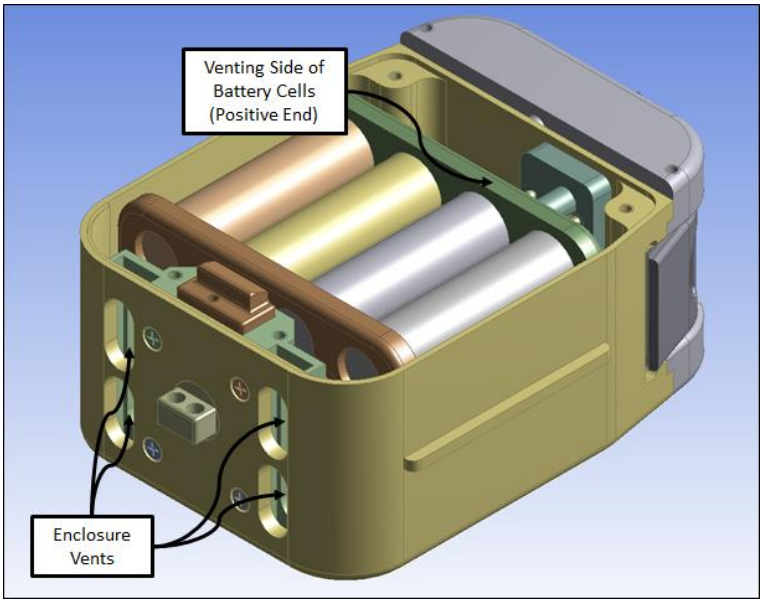

Figure 23. LPGT CAD model for CFD.

[11] ANSYS® DesignModeler™ is a trademark of ANSYS, Inc.
[12] ANSYS® Meshing™ is a trademark of ANSYS, Inc.
[13] ANSYS® Fluent® is a registered trademark of ANSYS, Inc.

E. LPGT CFD Results

Surface contour plots were created in order to illustrate the heat flux spatial distribution predicted by the model. It should also be noted that heat flux values greater than or equal to -2.5×10^{-5} W/m^2 have a magenta color, and therefore true maximum values are not shown. The first contour plot is shown in Figure 24 and illustrates the predicted surface heat flux values on the vent side of the battery cell. The venting cell (or trigger cell) is identified with a number "10", and all of the other cells have also been labeled. The contour plot shown in Figure 25 shows the predicted surface heat flux values for the non-vent side (negative terminals) of the battery cell. It should be noted that the heat flux scale in Figure 25 has been reduced by an order of magnitude vs. the data presented in Figure 24, which was done to reflect the lower heat transfer rates on the non-venting side. As mentioned previously, the heat fluxes from the CFD analysis were scaled to improved correlation between the model and the test data. Future CFD analysis efforts would focus on assessing the sensitivity of the predicted heat fluxes with different modeling assumptions (turbulence modeling, numerical schemes, numerical grids, etc.).

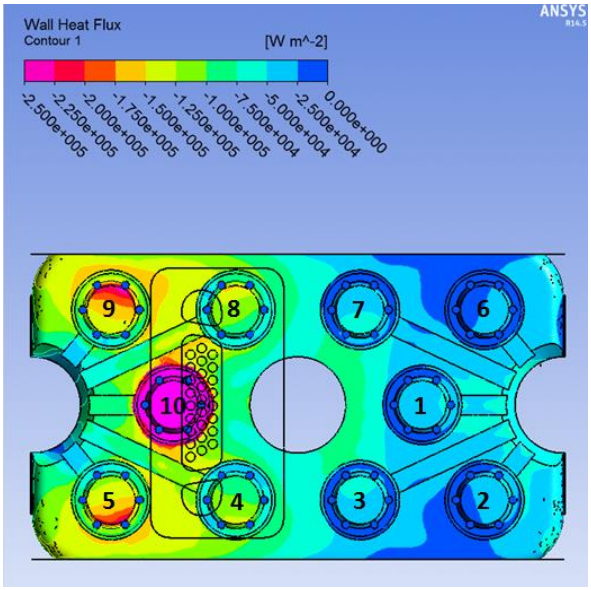

Figure 24. Wall heat-flux contour plot of battery cell venting side (positive terminals).

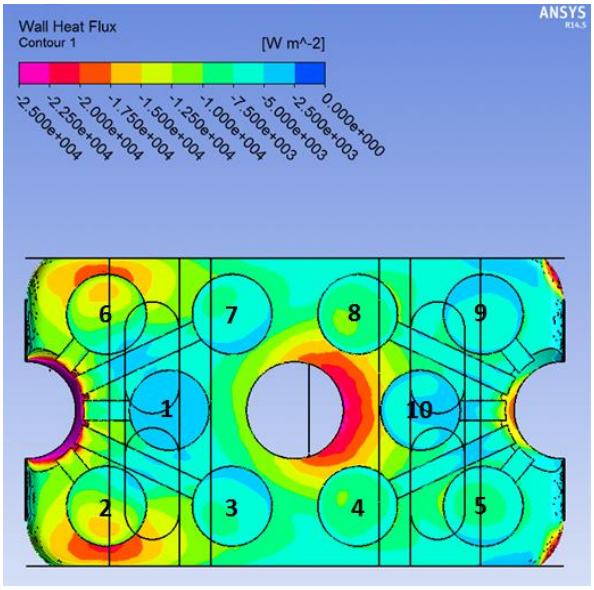

Figure 25. Wall heat-flux contour plot of battery cell non-venting side (negative terminals).

VI. Conclusions

Analysis and testing in support of further risk reduction in lithium-ion battery design is ongoing. Forward work includes analysis under vacuum conditions requiring removal of the air conduction network. However, a number of conclusions can be drawn from the first phase of this work, specifically:

1. Models showed good agreement with the experiments for single cells and battery pack configurations.
2. A cell heating factor correlated to experimental data is useful for expressing the fraction of energy liberated during a thermal runaway event that is released through the cell canister wall.
3. Direct cell-to-cell contact can lead to propagation of thermal runaway (TR) via direct heat conduction.
4. Effluents from cell venting carry sufficient energy to promote propagation of TR and must be managed.
5. CFD may be useful for evaluating the energy distribution of vent products, especially in regions of direct impingement.
6. Heat transfer through atmosphere present in the LREBA and LPGT battery enclosures is primarily via gas conduction. Free-space is too small to sustain convective heat transfer.
7. For the configurations tested, heat transfer through the cell can comprises, approximately, less than half of the cell's total energy.

8. The thermal resistance from the cell winding to the cell wall is a critical parameter in modeling of TR of lithium-ion cells and is in need of controlled test results to guide future models.
9. Adding a spreader to the LREBA design added a small amount of margin to the existing design.

Acknowledgments

The work described in this paper was sponsored by the NASA Engineering and Safety Center (NESC) under the leadership of Dr. Christopher Iannello and assessment leads Mr. Paul Shack of the TEAMS2 support to NESC and Mr. Robert Button of the NASA Glenn Research Center. Battery design iterations and testing were performed under the leadership of Dr. Eric Darcy of the NASA Johnson Space Center. Dr. Sean Rayman of the University of South Carolina is acknowledged for his work on the early internal cell models. The overall Computational Fluid Dynamics analysis was organized under the leadership of Dr. Cetin Kiris of the NASA Ames Research Center.

References

[1]Coman, T. P., White, R. & Rayman, S., "A Lumped Model of Venting During Thermal Runaway in a Cylindrical Lithium Cobalt Oxide Lithium-ion Cell," Journal of Power Sources, Vol. 307, 2016, pp.56 – 62.

[2]T. D. Hatchard, D. D. MacNeil, A. Basu and J. R. Dahn, "Thermal Model of Cylindrical and Prismatic Lithium-Ion Cells," Journal of the Electrochemical Society, Vol. 148 No. 7, 2001, A755-A761.

[3]Nancy Hall, "Isentropic Flow Equations", 2015, [online source], URL: https://www.grc.nasa.gov/www/k-12/airplane/isentrop.html

[4]Yunus Cengel, Fluid Mechanics Fundamentals and Applications, 3rd Edition, McGraw-Hill, 2006.

[5]Golubkov, A. W., Fuchs, D., Wagner, J., Wiltsche, H., Stangl, C., Fauler, G., Voitic, G., Thaler, A., Hacker, V., "Thermal-Runaway Experiments On Consumer Li-Ion Batteries With Metal-Oxide And Olivin-Type Cathodes." RSC Advances, Vol. 4, 2014, pp.3633-3642.

[6]Personal communication with the Applied Modeling and Simulation Branch at NASA Ames Research Center.